International Journal of Engineering Research and Development
e- ISSN: 2278-067X, p-ISSN: 2278-800X, www.ijerd.com
Volume 22, Issue 7 (July 2026), PP 172-180

A Labview-Based Localization and Navigation Algorithm for Mobile Robots

Yu Shao
Huaibei Mining Co., Ltd., Qinan Coal Mine
Huaibei, Anhui, China
Corresponding Author: Yu Shao

ABSTRACT: *With the rapid of robotics technology, autonomous mobile robots are increasingly used in industrial and service fields. Positioning and navigation system as the core component of mobile robot, its performance directly determines the robot's autonomy and intelligence level. In this paper, based on LabVIEW platform, combined with LMS100 laser sensor and reflector positioning technology, a set of high-precision and high-stability mobile robot positioning and navigation system is designed and realized. The system acquires data through laser scanning, and after clustering, matching and coordinate conversion, it calculates the real-time position of the robot using the three-side localization algorithm. The experimental results show that the positioning error of the system under static conditions is less than 15mm in the x and y directions respectively, which is required for industrial applications.*
KEY WORDS: *labview; mobile robot; localization and navigation; laser sensor; reflector; three-sided localization*

Date of Submission: 09-07-2026 Date of acceptance: 21-07-2026

I. INTRODUCTION

With the rapid of robotics technology, autonomous mobile robots are increasingly used in industrial and service fields, and high-precision localization and navigation technology is the key to realize their autonomous operation. However, the existing localization methods mostly rely on a single sensor and matching strategy, with insufficient adaptive and anti-interference capabilities in unstructured, and have not yet realized multi-source information fusion and robust position estimation under dynamics. Currently, the localization system still faces the challenge of insufficient stability and accuracy in complex dynamics. In this paper, to address this problem, we carry out the research of mobile robot localization method based on laser sensor and reflector.

In this paper, a six-degree-of-freedom mobile robot is used as a platform, which is scanned by LMS100 laser sensor, and a complete data processing and position solving system is developed by LabVIEW software. The guidelines for reasonable placement of reflectors are proposed, the functions of sensor communication, point cloud clustering, feature extraction and coordinate matching are realized, and the robot position is calculated by using the three-sided localization algorithm. Experiments show that the positioning error of the system under static conditions is less than 15 mm in both X and Y directions, which has good accuracy and reliability. This study provides an effective solution for high-precision localization of mobile robots under complexity, which is of reference significance for promoting the practicalization of related technologies.

II. MOBILE ROBOT POSITIONING SYSTEM PROGRAM DESIGN

2.1 Composition Of Mobile Robot Positioning System

The six-degree-of-freedom mobile robot platform studied in this project adopts Mecanum wheels to realize omnidirectional movement, and its chassis uniformly and symmetrically arranges four independently-driven wheels, each driven by a separate motor, and synergistically controlled by Peifu modules, so that the platform has the ability of in-plane three-degree-of-freedom movement, and the mobility flexibility and adaptability are significantly superior to that of the structure.

The localization system consists of a laser sensor and a reflector beacon. The laser sensor has become the core sensor for mobile robot positioning and navigation with its advantages of long detection distance, high measurement accuracy, high angular resolution and fast sampling rate. This system selects SICK's LMS100 2D laser sensor for real-time position estimation and navigation needs. Reflector selected for the SICK company supporting the special reflector, from which the energy value of the return beam is generally higher than that of other surrounding objects, to facilitate the extraction of data.

2.2 Laser Scanning Reflector Localization Algorithm

Laser scanning localization is the core technology for mobile robots to realize autonomous navigation, which provides the basis for path planning and behavioral decision-making by solving the real-time position of the robot in the global coordinate system.

2.2.1 Definition of the Coordinate System

The localization system is based on two coordinate systems: Global coordinate system: a fixed two-dimensional reference system (X, Y) based on the work site, where all the preset coordinates of the reflectors and the final position of the robot are based on. The position of the robot $p_0 = (X_0, Y_o, \alpha_0)^T$ is shown in Figure.1. Local coordinate system: the mobile coordinate system (X', Y') is fixedly connected to the robot body, the origin of which is located at the installation point of the laser sensor, and the X'-axis is pointing to the forward direction of the robot. This coordinate system measures the local coordinates ($X_S{}', Y_S{}', \theta$) of the reflector in real time, as shown in Figure.2.

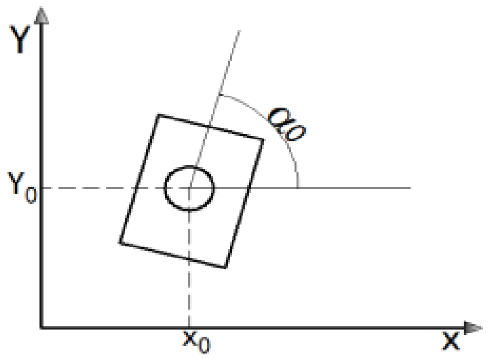

Figure.1 Global Coordinate System

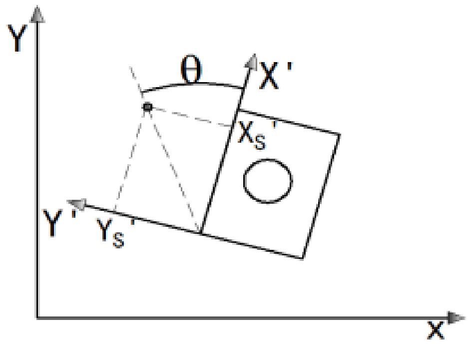

Figure.2 Local Coordinate System

The global coordinates and local coordinates of the preset reflector in the system there is a certain relationship, as shown in Figure. 3, set a preset reflector of the global coordinates (X_S, Y_S, α_S), the local coordinates of its measured ($X_S{}', Y_S{}', \theta$), at this time, the origin of the local coordinate system that is the location of the laser sensor installed in the global coordinate system coordinates ($X_0{}', Y_0', \alpha_0$), there are three such as the relationship between the formula 1.

$$\begin{Bmatrix} x_S = x_0' + x_S' \cos\alpha_0 - y_s' \sin\alpha_0 \\ y_s = y_0' + x_s' \sin\alpha_0 + y_s' \cos\alpha_0 \\ \alpha_s = \alpha_0 + \theta_s \end{Bmatrix} \quad (1)$$

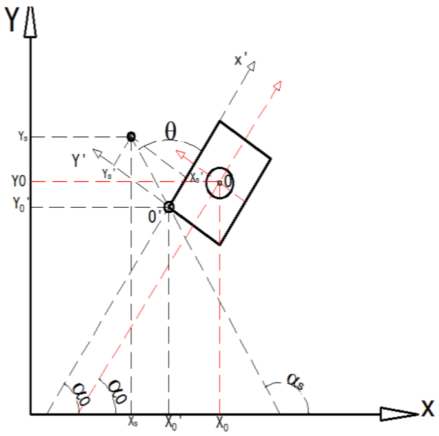

Figure.3 Relationship between Global and Local Coordinates

2.2.2 Principle of Laser Scanning Reflector Positioning Algorithm

The positioning algorithm is the core of the positioning system, which directly determines whether the acquired position is accurate. In this paper, we adopt the three-sided localization algorithm, as shown in Figure.4.

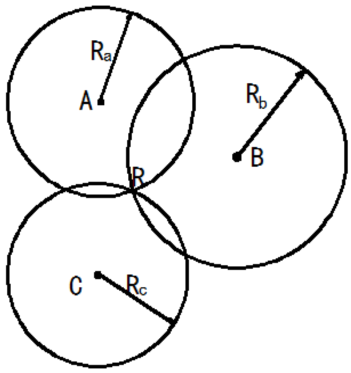

Figure.4 Three-sided Localization Algorithm

The position is solved by measuring the distance from the robot to at least three reflectors. A circle is made with the reflectors as the center and the measured distances as the radius, and its intersection point is the robot position. This method is efficient in calculation and simple in realization, and is adopted in this system. Based on the above principles, the overall dimensions of the reflectors in this project are designed as follows: height: 265mm diameter: 120mm, and the installation height of the laser sensor is 80mm from the ground.

III. Implementation of LabVIEW-based positioning algorithm

This chapter implements the positioning algorithm of six-degree-of-freedom mobile robot based on LabVIEW graphical, covering the whole process from sensor communication, data preprocessing, feature extraction to position solving. This chapter implements the positioning algorithm of six-degree-of-freedom mobile robot based on LabVIEW graphical, covering the whole process from sensor communication, data preprocessing, feature extraction to position solving.

3.1 Data Pre-Processing and Coordinate Conversion

The laser sensor is set to scan at an angle of 270° with a resolution of 0.5° , and 541 data points are acquired in a single scan. Each point is stored in polar coordinates, containing the distance ρ and energy value E. By coordinate conversion:

$$\left.\begin{cases} x_i = \rho_i \cos\theta_i \\ y_i = \rho_i \sin\theta_i \end{cases}\right\}(i = 1,2,3.....N) \tag{2}$$

The polar coordinates are converted to a right-angle coordinate system, which provides the basis for subsequent processing.

3.2 Point Cloud Clustering and Feature Extraction

Propose a clustering method based on energy thresholding and spatial proximity:

1. energy screening: set the energy threshold 180 to preliminarily screen the highly reflective points that

may come from the reflector.

2. Adaptive clustering: spatial clustering is performed using variable distance threshold ρ, and the threshold value adapts with the measurement distance:

$$\rho = r_{i-1}\left(\frac{\sin\Delta\phi}{\sin(\lambda-\Delta\phi)}\right)+3\sigma_r \tag{3}$$

where $\Delta\phi$ is the angular resolution of the laser sensor and λ is an auxiliary constant parameter.

3. Roundness detection: Introduce the roundness error index $\bar{d}$, establish the fitting model of $\bar{d}$ and the measured distance through experiments, and effectively distinguish the reflector from other highly reflective objects in the middle.

3.3 Extraction Exploration of Roundness Testing Conditions

In order to further determine the specific conditions of roundness detection, combined with the group's existing experimental equipment, first of all, a large number of experimental data collection, the overall idea: is to analyze and process the experimental data to derive the $\bar{d}$ and reflective plate placed in the distance or angle of the linear or nonlinear relationship between the $\bar{d}$ and the final use of $\bar{d}$ to express the roundness of this abstract concept. The data acquisition is as follows:

The measurement angle range is 240°, the measurement distance range is 2750mm, and the reflectors are placed in each direction in increments of 250mm, as shown in Figure.5.

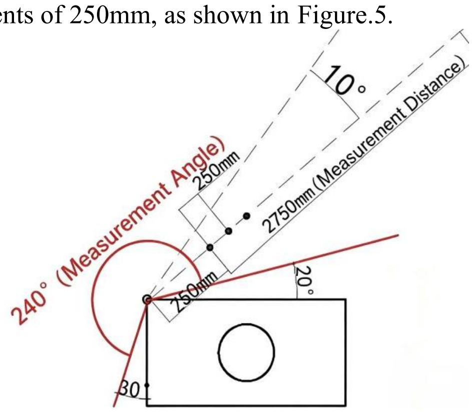

Figure.5 Schematic diagram of experimental data acquisition

Measured according to the above method, a total of 276 sets of experimental data were obtained, and each set of data contains information such as: current reflector placement distance, angle, extracted polar coordinates of the center of the reflector (C_r, C_θ), d_i, and $\bar{d}$.

After observing each set of data, it is found that the value of the points in $\bar{d}$ whose positions are closer to the two sides is larger, i.e., it indicates that the points closer to the two sides are not scanned as high as they should be, and the obtained $\bar{d}$ data is not reliable. Therefore, when calculating $\bar{d}$, it is reasonable to choose to delete the first and last n points, and then use the remaining data to calculate $\bar{d}$, which yields better results.

3.4 MATLAB processing of returned data

Using the actual positional parameters of the reflector placement as input (x=angle, y=distance). and $\bar{d}$ as output (z=$\bar{d}$), fit and a surface as shown in Figure.6 below.

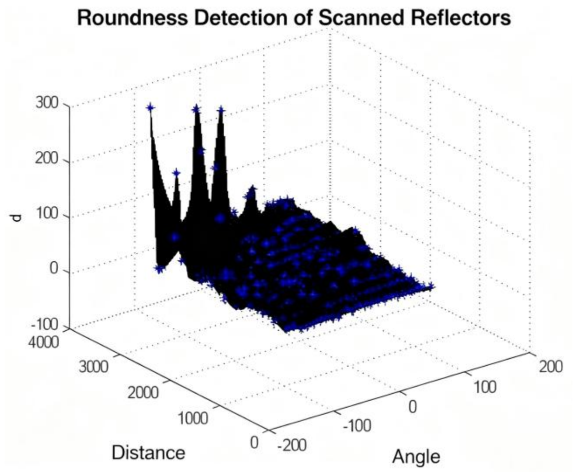

Figure.6 Fitting an image to the data

By rotating the view angle of the fitted image, as shown in Figure.7, observe and analyze to know that: the relationship between d and the angle of placement of the reflector is not large and can be ignored.

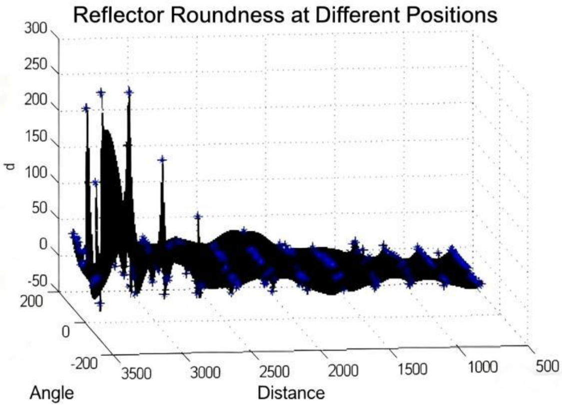

Figure.7 Fitting an image to the data

Similarly, by turning the view angle shown in Figure.8, observation and analysis know: d and reflector placement angle has a certain relationship, the farther the distance the greater d .

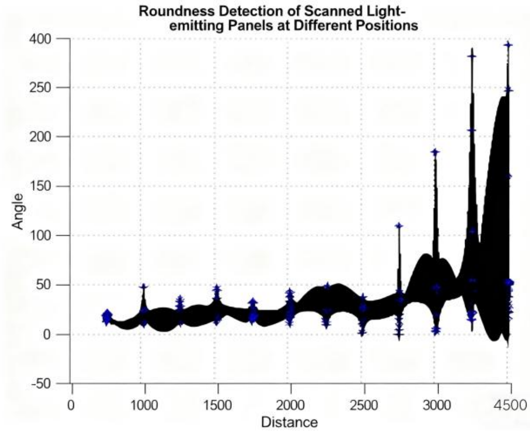

Figure.8 Fitting an image to the data

Through the above analysis, it is known that the value is mainly related to the distance of the reflector placement Figure.9 shows the two dimensional relationship between d and the distance distribution, and it can be seen that: with the distance, the d value appears to gradually increase the trend. According to Figure.9, it can also be found that the fluctuation range of d value is larger for the points corresponding to the distance after 3000mm.

Considering the effect of random error, in the linear fitting, the data selected for the distance of 750mm to 3000mm this range of data points, resulting in a linear equation for the green line in Figure.10, taking into account the range of data jump, will be fitted to the straight line and then upward translation of 30mm. the final translation of the linear equation as the roundness detection equation.

The general flow of roundness inspection conditions is shown in Figure.11.

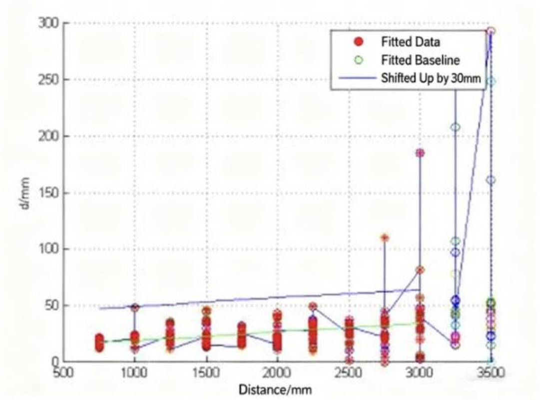

Figure.9 Two-dimensional plot of D and distance

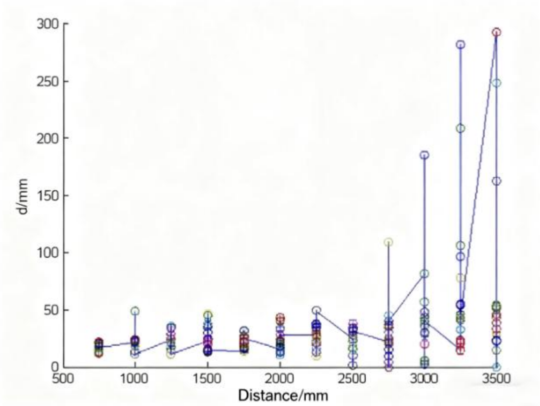

Figure.10 Linear fitting

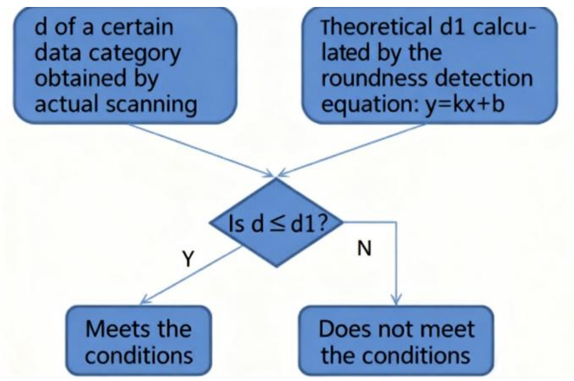

Figure.11 Roundness Inspection Flowchar

3.5 Matching of Reflective Boards

The data required for the final calculation of the mobile robot's pose is the coordinates of the reflective boards in the global coordinate system. However, the coordinates of the reflective boards obtained from laser scanning are only in the local coordinate system. Matching the reflective boards involves correlating the reflective boards in the local coordinate system to the global coordinate system. Therefore, the correctness of the reflective board matching has a significant impact on the accuracy of the positioning system, making it a crucial part of the overall positioning algorithm.

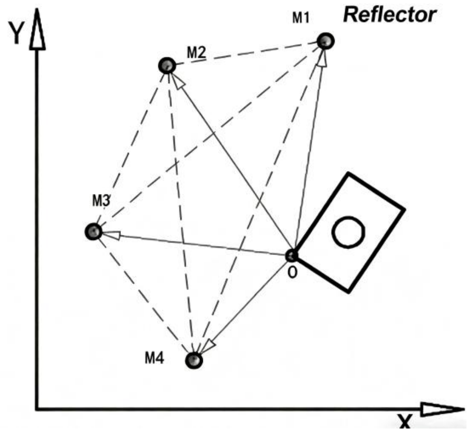

Figure.12 Schematic diagram of laser scanning once

Figure.12 shows the list of reflective panels obtained from the laser sensor scanning around. Assuming that the laser sensor obtains coordinates for four reflective panels during the scan, labeled as M_1、M_2、M_3、M_4, these will form C_4^3 triangles. For each triangle, the maximum angle and the lengths of the two sides forming this maximum angle will be calculated. For instance, for triangle $\Delta_{M_1M_2M_3}$, the lengths of M_1M_2、M_2M_3 as well as the angle $\angle M_1M_2M_3$ will be computed. Then, the parameters of the triangles just calculated will be compared one by one with each triangle formed by the preset global coordinates of the reflective panels. If the parameters of the two triangles are approximately equal within a certain error range, it is assumed that these two triangles are formed by the same three reflective panels, thus yielding the corresponding reflective panel coordinates in the global coordinate system.

3.6 Pose estimation of mobile robots

(1) Calculation of mobile robot posture

According to the principles of the three-sided positioning algorithm presented in Section 3 of Chapter 2, a mobile robot requires at least the coordinate information of three reflectors to determine its own position and orientation. Finally, the intersection points are obtained by establishing the equations of circles. The specific algorithm is as follows:

First, establish the equations of n circles:

$$\left\{\begin{array}{l}(X_1-X_0^{'})^2+(Y_1-Y_0^{'})^2=R_1^{\ 2}\\(X_2-X_0^{'})^2+(Y_2-Y_0^{'})^2=R_2^{\ 2}\\(X_3-X_0^{'})^2+(Y_3-Y_0^{'})^2=R_3^{\ 2}\\\cdots\cdots\\(X_i-X_0^{'})^2+(Y_i-Y_0^{'})^2=R_i^{\ 2}\\\cdots\cdots\\(X_n-X_0^{'})^2+(Y_n-Y_0^{'})^2=R_n^{\ 2}\end{array}\right\} \tag{4}$$

Select any two equations from formula 4 and subtract them to get a linear equation in $\left(X_0^{'},Y_0^{'}\right)$. By subtracting in pairs, you will obtain a linear system of equations in C_n^2. It can be observed that this is an over-constrained system of equations, so the least squares method is chosen to solve it. In the end, the position $\left(X_0^{'},Y_0^{'}\right)$ of the origin of the local coordinate system in the global coordinate system is calculated.

According to Figure.13, it can be seen that the orientation of the local coordinate system axis $O^{'}X^{'}$ is consistent with the orientation of the moving platform in the global coordinate system, with an angle of α_0 between them, which can be calculated using Formula 4.

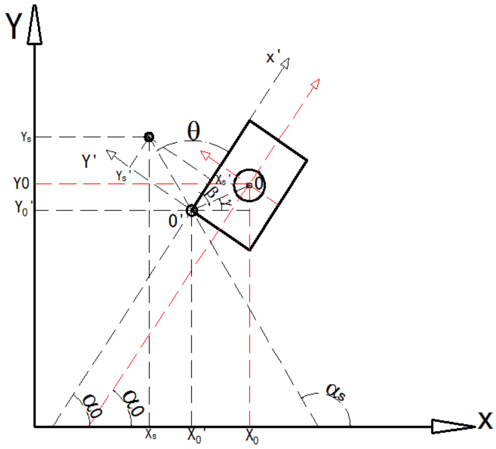

Figure.13 Coordinate relationship diagram

By

$$\alpha_o = \alpha_s - \theta = \arctan \frac{Y_S - Y_0^{'}}{X_S - X_O^{'}} - \theta \tag{5}$$

there will be:

$$\alpha_i = \arctan \frac{Y_i - Y_0{'}}{X_i - X_0^{'}} - \theta_i \tag{6}$$

Where $\alpha_{1,}\alpha_2 \ldots \alpha_i -$ is the orientation angle calculated based on the $1,2 \cdots i$ reflective board scanned; $(\theta_1, \theta_2 \cdots \theta_i) -$ is the orientation angle of the $1,2 \cdots i$ reflective board scanned by the light sensor in the local coordinate system; $(X_i, Y_i) -$ represents the position of the $1,2 \cdots i$ reflective board scanned in the global coordinate system; $(X_0{'}, Y_0{'}) -$ is the coordinates of the origin of the local coordinate system in the global coordinates;

The angle α_0 of the moving platform in the global coordinate system calculated from equation 6 is:

$$\alpha_0 = \frac{1}{n} \sum_{i=1}^{n} \alpha_i \tag{7}$$

(2) Calculation of the position coordinates of mobile robots

As shown in Figure.13, the origin of the local coordinate system in this project is located at the left rear corner of the mobile platform's body, rather than at the center of the mobile platform. Therefore, the actual position $(X_0^{'}, Y_0^{'})$ of the calculated local coordinate origin must be transformed to obtain the robot's position (X_0, Y_0). The specific calculation formula is as follows.

$$\begin{Bmatrix} X_0 = X_0^{'} + OO^{'} \cos(\gamma) = X_0^{'} + OO^{'} \cos(\alpha_0 - \beta) \\ Y_0 = Y_0^{'} + OO^{'} \sin(\lambda) = Y_0^{'} + OO^{'} \sin(\alpha_0 - \beta) \end{Bmatrix} \tag{8}$$

In the formula: α_0 is the robot's position angle, and α_0 is related to the dimensions of the mobile platform. Based on the above, the pose $P_0 = (X_0, Y_0, \alpha_0)^T$ of the mobile robot in the global coordinate system can be calculated.

IV. Experimental performance analysis of positioning algorithms

To evaluate the performance of the positioning system, the robot was placed in 10 different known positions under static conditions, with 3 measurements taken for each position. By comparing the coordinates obtained from the laser scanning with the actual coordinates, the positioning error was determined.

Table 1 Experimental data under static conditions

Number	Measured Value (mm)			Actual Value (mm)	$(\Delta x_{\max}, \Delta y_{\max})$
1	(755，1010)	(738，1009)	(762，1013)	(750，1000)	(12，13)
2	(758，2011)	(741，2012)	(767，1986)	(750，2000)	(17，14)
3	(760，2989)	(756，3009)	(739，3015)	(750，3000)	(11，15)
4	(1507，1011)	(1510，1009)	(1488，1015)	(1500，1000)	(12，15)
5	(1520，2009)	(1491，2007)	(1506，2010)	(1500，2000)	(20，10)
6	(1494，3007)	(1506，3011)	(1508，3010)	(1500，3000)	(8，11)
7	(2560，1015)	(2507，1008)	(2490，1013)	(2500，1000)	(10，15)
8	(2514，2017)	(2523，2008)	(2509，2004)	(2500，2000)	(23，17)
9	(2515，3001)	(2490，3018)	(2512，3011)	(2500，3000)	(15，18)
10	(3016，1019)	(3011，1013)	(3012，1015)	(3000，1000)	(16，19)

According to the data in Table 1, $(\Delta\bar{x}_{\max}, \Delta\bar{y}_{\max}) = (14.3, 14, 7)$ was derived.

The results indicate that the average positioning error of the system in the X direction is 14.3 mm and in the Y direction is 14.7 mm, which meets the positioning accuracy requirements for mobile robots.

V. Summary

This article designs and implements a six-degree-of-freedom mobile robot positioning system based on LabVIEW and laser sensors, aiming to solve the problem of high-precision pose estimation for mobile robots in complex environments. By analyzing the development status and key technologies of mobile robots, a solution using reflective panels as beacons and a trilateral positioning algorithm is proposed. The system utilizes the LMS100 laser sensor to scan the environment, and through the LabVIEW platform, it completes data collection, coordinate transformation, point cloud clustering, circularity detection, and reflective panel matching processing workflows to achieve real-time solving of the robot's pose. In addition, a dedicated LMS debugging interface was developed, which verified the system's positioning accuracy under static conditions, with average errors of less than 15mm in the x and y directions, indicating that the system is stable and reliable, meeting practical application needs.

REFERENCES

[1]. G. Chen, B. Wang, Y. Wang, et al., "A Survey on Mobile Robotic Technologies: Trends, Challenges and Future Directions," *Robotics and Autonomous Systems*, vol. 158, p. 104245, 2022.

[2]. H. Wang, Z. Li, Y. Pan, et al., "Advances and Trends in Robotic Intelligence: A Review from a Chinese Perspective," *Science China Information Sciences*, vol. 65, no. 12, p. 221201, 2022.

[3]. H. Durrant-Whyte and T. Bailey, "Simultaneous Localization and Mapping: Part I," *IEEE Robotics & Automation Magazine*, vol. 26, no. 2, pp. 99-110, June 2019.

[4]. A. Geiger, P. Lenz, C. Stiller, et al., "Vision for Intelligent Vehicles and Applications: A Survey," *IEEE Transactions on Intelligent Transportation Systems*, vol. 23, no. 7, pp. 7402-7415, July 2022.

[5]. C. Cadena, L. Carlone, H. Carrillo, et al., "Past, Present, and Future of Simultaneous Localization and Mapping: Toward the Robust-Perception Age," *IEEE Transactions on Robotics*, vol. 32, no. 6, pp. 1309-1332, Dec. 2019.

[6]. B. He, Y. Li, X. Wu, et al., "Deep Learning-Based Visual Navigation for Agricultural Mobile Robots in Unstructured Environments," *Computers and Electronics in Agriculture*, vol. 201, p. 107292, 2022.

[7]. F. Gao, S. Wu, J. Li, et al., "A Comprehensive Review of Navigation Methods and System Integration for Agricultural Mobile Robots," *AgriEngineering*, vol. 5, no. 1, pp. 1-22, 2023.

[8]. X. Si and Z. Wang, "Recent Advances in Multi-Sensor Fusion for Mobile Robots: State of the Art and Challenges," *IEEE Sensors Journal*, vol. 21, no. 19, pp. 21283-21294, 2021.

[9]. X. Xie, F. Cha and G. Li, "Advanced Localization Algorithms for Mobile Robots in Unknown and Dynamic Environments: A Review," *IEEE/CAA Journal of Automatica Sinica*, vol. 8, no. 5, pp. 967-989, 2021.

[10]. Z. Zheng, R. Xiong and D. Gu, "Integrated Navigation and Localization for Mobile Robots: Recent Methodologies and Applications," *Journal of Intelligent & Robotic Systems*, vol. 103, no. 3, p. 47, 2021.

[11]. BAIL EY T. Mobile robot localization and mapping in extensive outdoor environment [D]. Sydney: University of Sydney, 2002.

[12]. Einsele T. Real-time self-localization in unknown indoor environments using a panorama laser range finder [J].Proceedings of the 1997 IEEE International Conference on Intelligent Robots and Systems.1997,697-702

[13]. BAIL EY T. Mobile robot localization and mapping in extensive outdoor environment[D]. Sydney: University of Sydney, 2002.

[14]. L.Huang,W.Yu , S.K. Jhajharia. Speed Control of Differentially Driven Wheeled Mobile Robots-Tracking and Synchronization. IEEE Instrumentation Measurement Technology Conference, 2003.5:1407-1410.